

Mixing Distributions within the Quasi-Gaussian Entropy Theory: Multistate Thermal Equations of State Valid for Large Temperature Ranges

M. E. F. Apol[†] and A. Amadei^{*‡}

Groningen Biomolecular Sciences and Biotechnology Institute (GBB), Department of Biophysical Chemistry, University of Groningen, Nijenborgh 4, 9747 AG Groningen, The Netherlands, Department of Chemical Sciences and Technology, University of Rome "Tor Vergata", Via della Ricerca Scientifica 1, 00133 Rome, Italy

Received: August 29, 2002; In Final Form: December 3, 2002

In this article the quasi-Gaussian entropy (QGE) theory has been extended toward statistical-mechanical models that describe the temperature dependence of thermodynamic properties of fluids at fixed density over a very large temperature range, up to 15 times the critical temperature. The system's phase space is divided into multiple regions, each of which has a "potential" energy distribution that can be described by a simple model, e.g., a Gamma distribution. The overall "potential" energy distribution, which is directly related to the residual Helmholtz free energy of the system, then is a "mixture" of Gamma distributions, each with, for example, a different value of the "minimum" potential energy. Several such multistate models for the free energy were derived and tested on a series of small molecules at various densities: the hard core Yukawa fluid, the Lennard-Jones fluid, argon, methane, ammonia, water, and the extended simple point charge (SPC/E) water model. In almost all systems, a Gamma mixture of Gamma distributions provides a very accurate thermal model over a large temperature range starting at the coexistence line and applicable from ideal gas to dense liquid, even in the vicinity of the critical point. The shape of the "potential" energy distribution and its density dependence reflects the underlying molecular interactions, which are discussed by comparing different systems.

1. Introduction

Knowledge of thermodynamics and phase equilibria forms the basis of modern chemical process design. Accurate equations of state (EOS) are therefore an essential tool, and very many empirical and (semi)theoretical EOS have been proposed; see, e.g., the review by Sengers et al.¹ In the past decades, tremendous progress has been achieved in the development of EOS for fluid systems, based on statistical mechanics. An example is the statistical associating fluid theory (SAFT),^{2,3} which is basically derived from a hard-body equation of state with (relatively simple) intermolecular model potentials for hydrogen bonding and dispersion, included via perturbation theory. Specific knowledge on the systems enters via "molecular" parameters within the EOS, such as hard-sphere radii, dipole moments, etc. On the more empirical side, Wagner and co-workers for example have developed a sophisticated method to correlate experimental data using a "bank" of polynomial-like terms for the residual free energy.⁴ This procedure has been successfully used to generate thermodynamic tables of various systems, e.g., argon,⁵ methane,⁶ carbon dioxide,⁷ water,⁸ etc. In this case the parameters of the EOS are not directly related to molecular properties.

Recently, a new statistical-mechanical approach has been proposed, the quasi-Gaussian entropy (QGE) theory, which yields (thermal) equations of state based on knowledge of the distribution of macroscopic (energy) fluctuations in the system.^{9–11} By using some (relatively simple) "quasi-Gaussian" distribu-

tion¹² as a model based on general physical principles, an analytical expression of the (residual) free energy is obtained. Parameters are directly related to thermodynamic properties at one arbitrary state point. Already a mathematically simple model like the Gamma distribution provides an analytical expression that accurately describes the thermal properties of, e.g., water and the Lennard-Jones fluid over a considerable temperature range.^{9,13–15} Extensions toward more sophisticated model distributions resulted in so-called "multistate models", where the system's phase space is divided into several parts, each being described by different (simple) model distributions. Examples are the double and triple Gamma state model for ideal gas molecules,¹⁶ and the double state temperature¹⁴ and polarization/magnetization models¹² for macroscopic systems.

In this article we present for the first time a general derivation of such thermal multistate models with an arbitrary number of states. The corresponding (energy) distributions turn out to be equivalent to the "mixing distributions" that are known from the statistical literature.¹⁷ Several continuous and discrete "mixtures" will be derived and the corresponding thermal EOS applied to a range of different fluids that vary strongly in polarity: argon, methane, ammonia, water, etc. Especially the Gamma mixture of Gamma states provides a very accurate description of the thermal behavior of these systems over a very large temperature range, i.e., up to 15 times the critical temperature.

2. Theory

In the canonical ensemble, the excess or confined ideal reduced Helmholtz free energy A^* is defined as^{9,11,16,18}

* To whom correspondence should be addressed. E-mail: andrea.amadei@uniroma2.it.

[†] University of Groningen.

[‡] University of Rome "Tor Vergata".

$$A^* = -kT \ln \left\{ \frac{Q}{Q_{*ref}} \right\} \quad (1)$$

where Q and Q_{*ref} are the partition functions of the actual system and of the reference state. The reference system is, as explained in previous articles,^{9,13,16} an “ideal gas” at the same temperature and density without any semiclassical inter- and intramolecular potential energy, confined within the same part of phase space as the actual system. Because of “excluded volume” effects, only a part of the phase space with volume fraction ϵ is accessible to the system, at least within the temperature range of interest (see Figure 1a,b). This confinement gives an extra, purely entropic contribution to the ideal reduced free energy A' , i.e., with respect to an “ideal gas” without any semiclassical potential energy that can have (fully) overlapping atoms.^{9,11,16,18}

$$A' = -kT \ln \left\{ \frac{Q}{Q_{ref}} \right\} = A^* - kT \ln \epsilon \quad (2)$$

If there is no excluded volume effect, $\epsilon = 1$ and both free energies are equal. For small molecules such as the Lennard-Jones (LJ) fluid and water, the confinement can be well modeled by a hard-sphere EOS.^{9,15,18,19} The “potential” energy and its temperature derivatives are not affected by the confinement: $U' = U^*$, $C'_V = C^*_{V}$, etc. For small molecules without semiclassical internal degrees of freedom (like argon, water, ammonia, and methane), A' is equal to A^* , the reduced or residual free energy with respect to a usual ideal gas at the same temperature and density.⁹

The ratio Q_{*ref}/Q can be written as the moment generating function^{17,20} (MGF) of the probability distribution function $\rho(\mathcal{U}')$ of the “potential” energy \mathcal{U}' of the system:⁹

$$\frac{Q_{*ref}}{Q} = \langle e^{\beta \mathcal{U}'} \rangle \equiv G_{\mathcal{U}'}(\beta) = \int e^{\beta \mathcal{U}'} \rho(\mathcal{U}') d\mathcal{U}' \quad (3)$$

Alternatively, it can also be expressed as the MGF of the distribution $\rho_{ref}(\mathcal{U}')$ in the reference ensemble:

$$\frac{Q}{Q_{*ref}} = \langle e^{-\beta \mathcal{U}'} \rangle_{ref} \equiv G_{\mathcal{U}'}^{ref}(-\beta) = \int e^{-\beta \mathcal{U}'} \rho_{ref}(\mathcal{U}') d\mathcal{U}' \quad (4)$$

As explained previously,¹⁰ this latter expression provides a more direct route to the free energy, as the parameters of $\rho_{ref}(\mathcal{U}')$ are temperature independent, whereas the parameters of $\rho(\mathcal{U}')$ are implicitly dependent on temperature, and the full temperature dependence of A^* is in that case only obtained after solving the so-called thermodynamic master equation.^{9,13} In this paper we will use the reference distribution representation, eq 4.

In previous articles we used relatively simple model distributions to obtain the complete thermodynamics, i.e., the *statistical state* of the system. Using a Gamma distribution, for example, we thus obtained the Gamma state that was successfully applied to, e.g., water^{9,18} and the LJ fluid^{15,19} over a considerable temperature range. However, a single Gamma distribution is not accurate enough to describe the thermodynamics of the LJ fluid over a very large temperature range (10–15 times the critical temperature). Therefore, an improved model has been developed¹⁵ that describes the major part of the accessible part of phase space by a single Gamma distribution and treats the remaining part as a perturbation; see Figure 1c. This formed the basis of a complete equation of state for the LJ fluid.

In this article, instead of directly modeling the accessible part of phase space by one (relatively simple) model distribution, we split the accessible part of phase space of the system, as

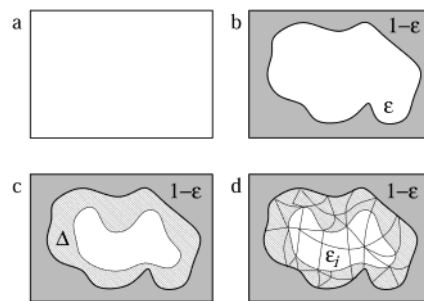


Figure 1. Schematic view of phase space: (a) “ideal gas” phase space; (b) confinement to a fraction ϵ due to excluded volume effects; (c) confinement and a perturbation region Δ within the accessible part of phase space; (d) confinement and division of the accessible part of phase space into multiple regions i with fractions ϵ_i .

well as that of the reference state, into a number of regions $i = 1, \dots, n$ (see Figure 1d) in such a way that the thermodynamics inside each region is at every temperature given by one unique simple statistical state.^{14,16}

$$Q = \sum_{i=1}^n Q_i \quad (5)$$

$$Q_{*ref} = \sum_{i=1}^n Q_{*ref,i} \quad (6)$$

The excess free energy is therefore given by

$$\begin{aligned} A^*(T) &= -kT \ln \left\{ \sum_{i=1}^n \frac{Q_i}{Q_{*ref,i}} \frac{Q_{*ref,i}}{Q_{*ref}} \right\} = \\ &= -kT \ln \left\{ \sum_{i=1}^n \epsilon_i \langle e^{-\beta \mathcal{U}'} \rangle_{ref,i} \right\} \\ &= -kT \ln \left\{ \sum_{i=1}^n \epsilon_i e^{-\beta A_i^*} \right\} = A_1^*(T) - kT \ln \left\{ \sum_{i=1}^n \epsilon_i e^{-\beta \Delta A_i^*} \right\} \end{aligned} \quad (7)$$

where $\epsilon_i = Q_{*ref,i}/Q_{*ref}$ is the temperature independent volume fraction of region i with $\sum_i \epsilon_i = 1$, A_i^* is the confined ideal reduced free energy of region i and $\Delta A_i^* = A_i^* - A_1^*$ is the free energy difference with respect to some (arbitrarily chosen) region 1.

Each region i with free energy

$$A_i^* = -kT \ln \langle e^{-\beta \mathcal{U}'} \rangle_{ref,i} = -kT \ln \int e^{-\beta \mathcal{U}'} \rho_{ref,i}(\mathcal{U}'; \alpha_i) d\mathcal{U}' \quad (8)$$

can be described by a specific statistical state, defined by some type of distribution $\rho_{ref,i}(\mathcal{U}'; \alpha_i)$ and set of parameters α_i . Assuming that all regions can be described by the same *type* of distribution $\rho_{ref}(\mathcal{U}')$ but with different parameters, we can sum over all possible parameter sets $\{\alpha\}$ instead of regions i . Hence eq 7 can be rewritten as

$$\begin{aligned} A^*(T) &= -kT \ln \left\{ \sum_{\{\alpha\}} p_\epsilon(\alpha) e^{-\beta A^*(T; \alpha)} \right\} \\ &= A^*(T; \alpha_1) - kT \ln \left\{ \sum_{\{\Delta\alpha\}} p_\epsilon(\Delta\alpha) e^{-\beta \Delta A^*(T; \Delta\alpha)} \right\} \end{aligned} \quad (9)$$

where $p_\epsilon(\alpha)$ is the multivariate (temperature independent) discrete probability distribution of a certain parameter set α , $\Delta\alpha = \alpha - \alpha_1$ with α_1 a yet unspecified set of parameter values,

$A^*(T; \alpha) = -kT \ln \int e^{-\beta \mathcal{U}'} \rho_{\text{ref}}(\mathcal{U}'; \alpha) d\mathcal{U}'$, and $\Delta A^*(T; \Delta \alpha) = A^*(T; \alpha) - A^*(T; \alpha_1)$.

Note that the magnitude of the difference in free energy for different parameter sets $\Delta A^*(T; \Delta \alpha)$ with respect to kT determines if the system gradually changes parameters or if a ‘‘macroscopic’’ phase transition occurs when the temperature is altered. If the system consists of ‘‘isolated’’ single molecules (i.e., ideal gas condition), $\Delta A^*(T; \Delta \alpha) \sim \mathcal{O}(kT)$, and so no phase transition takes place; see Amadei et al.¹⁶ Similarly, a multistate Gaussian approach was used by Hummer et al.²¹ to calculate by Monte Carlo simulations the change in electrostatic solvation free energy of a solute molecule, with $n = 6$ or 8 . Also in that case $\Delta A^*(T; \Delta \alpha) \sim \mathcal{O}(kT)$. On the other hand, for the electromagnetic double state models of Apol et al.,¹² where the free energy change is $\mathcal{O}(NkT)$, a macroscopic phase transition does occur.

In the limit that the gaps between parameter values are differentials, eq 9 becomes

$$A^*(T) = A^*(T; \alpha_1) - kT \ln \int \rho_\epsilon(\Delta \alpha) e^{-\beta \Delta A^*(T; \Delta \alpha)} d\Delta \alpha \quad (10)$$

where $\rho_\epsilon(\Delta \alpha)$ is the multivariate continuous probability distribution of the parameters $\Delta \alpha$. This distribution is by definition also temperature independent, but implicitly dependent on density.

Without loss of generality we can define state 1 by the set of average parameters: $\alpha_1 = \langle \alpha \rangle_\epsilon = \sum_{\{\alpha\}} p_\epsilon(\alpha) \alpha$ or $\int \rho_\epsilon(\alpha) \alpha d\alpha$ where $\langle \cdot \rangle_\epsilon$ denotes an average over the parameter distribution (not to be confused with the ensemble average, eq 3); hence $\Delta \alpha = \alpha - \langle \alpha \rangle_\epsilon$ are the parameter fluctuations around the mean parameter values. Note that ΔA^* may also depend on α_1 ; however, for brevity we will simply write $\Delta A^*(T; \Delta \alpha)$. The domain of each (fluctuating) parameter is determined by physical and mathematical restrictions. For example, in the case of a positive Gamma state (see eq 16), one of the parameters is the minimum energy $\mathcal{U}'_{\text{min}}$. Clearly, there must be an overall minimum energy $\mathcal{U}'_{\text{MIN}}$, so $\mathcal{U}'_{\text{MIN}} \leq \mathcal{U}'_{\text{min}}$. Furthermore, the probability distributions $p_\epsilon(\Delta \alpha)$ and $\rho_\epsilon(\Delta \alpha)$ must be such that the sum and integral in eqs 9 and 10 are finite.

The overall energy distribution in the reference condition, $\rho_{\text{ref}}(\mathcal{U}')$, is simply given by the average

$$\begin{aligned} \rho_{\text{ref}}(\mathcal{U}') &= \langle \rho_{\text{ref}}(\mathcal{U}'; \alpha) \rangle_{\text{ref}} = \langle \rho_{\text{ref}}(\mathcal{U}'; \alpha) \rangle_\epsilon \\ &= \sum_{\{\alpha\}} p_\epsilon(\alpha) \rho_{\text{ref}}(\mathcal{U}'; \alpha) \\ &= \int \rho_\epsilon(\alpha) \rho_{\text{ref}}(\mathcal{U}'; \alpha) d\alpha \quad (11) \end{aligned}$$

In the statistical literature,¹⁷ $\rho_{\text{ref}}(\mathcal{U}')$ is known as a ‘‘mixing distribution’’, as it can be regarded as a ‘‘mixture’’ of distributions $\rho_{\text{ref}}(\mathcal{U}'; \alpha)$ of the same type with different parameter values, mixed according to a parameter distribution $p_\epsilon(\alpha)$ or $\rho_\epsilon(\Delta \alpha)$. It must be stressed that the potential energy distribution of the reference state $\rho_{\text{ref}}(\mathcal{U}')$ is temperature independent; however, the corresponding distribution of the actual system $\rho(\mathcal{U}')$ does depend on temperature.¹⁴

$$\begin{aligned} \rho(\mathcal{U}') &= \langle \rho(\mathcal{U}'; \alpha) \rangle = \frac{\sum_{\{\alpha\}} \rho(\mathcal{U}'; \alpha) p_\epsilon(\alpha) e^{-\beta A^*(T; \alpha)}}{\sum_{\{\alpha\}} p_\epsilon(\alpha) e^{-\beta A^*(T; \alpha)}} \\ &= \frac{\int \rho(\mathcal{U}'; \alpha) \rho_\epsilon(\alpha) e^{-\beta A^*(T; \alpha)} d\alpha}{\int \rho_\epsilon(\alpha) e^{-\beta A^*(T; \alpha)} d\alpha} \quad (12) \end{aligned}$$

Furthermore, the parameter distributions $p_\epsilon(\alpha)$ and $\rho_\epsilon(\alpha)$ are by definition temperature independent, whereas the probability of observing the system in a state characterized by a specific parameter set α is (cf. eq 12) again a function of T . $p_\epsilon(\alpha)$ and $\rho_\epsilon(\alpha)$ can therefore also be interpreted as the probability distributions of finding the system in a state α at infinite temperature. Hence, the ensemble average $\langle \cdot \rangle_{\text{ref}}$ corresponds to the parameter average $\langle \cdot \rangle_\epsilon$; see also eq 11.

Clearly, for the mixing distribution $\rho_{\text{ref}}(\mathcal{U}')$ the overall moment generating function $G_{\mathcal{U}'}^{\text{ref}}(-\beta) = \langle e^{-\beta \mathcal{U}'} \rangle_{\text{ref}}$ is a mixture of the MGFs of the ‘‘basic’’ distributions $\tilde{G}_{\mathcal{U}'}^{\text{ref}}(-\beta; \alpha) = \int e^{-\beta \mathcal{U}'} \rho_{\text{ref}}(\mathcal{U}'; \alpha) d\mathcal{U}'$:

$$\begin{aligned} G_{\mathcal{U}'}^{\text{ref}}(-\beta) &= \sum_{\{\alpha\}} p_\epsilon(\alpha) \tilde{G}_{\mathcal{U}'}^{\text{ref}}(-\beta; \alpha) \\ &= \int \rho_\epsilon(\alpha) \tilde{G}_{\mathcal{U}'}^{\text{ref}}(-\beta; \alpha) d\alpha \quad (13) \end{aligned}$$

Note that the previously derived thermal equations of state for quantum-mechanical systems (solids)²² can be considered as a special case of the general approach described above. In that case the MGF of the (discrete) energy distribution $G_{\epsilon_L}^0(-\Delta \beta) = \prod_i \tilde{g}_{\epsilon_{iL}}^0(-\Delta \beta; \alpha)$ was assumed to be the *product* of N MGFs of ‘‘basic’’ distributions with different parameters α (i.e., the energy gap $\Delta \epsilon$), so that the cumulant generating function^{17,20} (CGF) $K_{\epsilon_L}^0$

$$\begin{aligned} K_{\epsilon_L}^0(-\Delta \beta) &\equiv \ln G_{\epsilon_L}^0(-\Delta \beta) = N \sum_{\{\alpha\}} p_\epsilon(\alpha) \ln \tilde{g}_{\epsilon_{iL}}^0(-\Delta \beta; \alpha) \\ &= N \int \rho_\epsilon(\alpha) \ln \tilde{g}_{\epsilon_{iL}}^0(-\Delta \beta; \alpha) d\alpha \quad (14) \end{aligned}$$

is a mixture of the CGFs of the basic distributions $\tilde{k}_{\epsilon_{iL}}^0 = \ln \tilde{g}_{\epsilon_{iL}}^0$. As explained in ref 22, this corresponds to a special ‘‘clustering’’ of the physical states of the system, such that the partition function can be factorized in an inhomogeneous way. This inhomogeneous factorization cannot be correct in the infinite temperature limit. However, for solids with finite melting temperature this is a good approximation. The completely general splitting of phase space according to eqs 5 and 6 is correct even in the infinite temperature limit.

The simplest possible distribution for the parameters is a multivariate single state discrete distribution or a multivariate Dirac delta function, for which eq 10 simply reduces to the single statistical state defined by the average parameters. As a more complicated model we can assign a nontrivial distribution to one of the parameters, $\Delta \alpha_1$, e.g. and assume that the distributions of the remaining $p - 1$ parameters are so ‘‘narrow’’ around the average, that they still can be modeled as fixed:

$$\begin{aligned} p_\epsilon(\Delta \alpha) &= p_\epsilon(\Delta \alpha_1) \prod_{j=2}^p \delta_{\Delta \alpha_j} \\ \rho_\epsilon(\Delta \alpha) &= \rho(\Delta \alpha_1) \prod_{j=2}^p \delta_D(\Delta \alpha_j) \quad (15) \end{aligned}$$

3. Statistical States

The simple Gamma statistical state is rather successful in describing the thermodynamics of both polar and apolar fluids over a considerable temperature range. The model distribution $\rho_{\text{ref}}(\mathcal{U}')$ is for a simple Gamma state a three-parameter Gamma distribution:^{20,23}

$$\rho_{\text{ref}}(\mathcal{U}') = \frac{|\theta|\theta^{a-1}}{\Gamma(a)} (\mathcal{U}' - \mathcal{U}'_x)^{a-1} e^{-\theta(\mathcal{U}' - \mathcal{U}'_x)} \quad (16)$$

where \mathcal{U}'_x is some extreme excess energy value. For a *positive* Gamma distribution, $\theta > 0$, $\mathcal{U}'_x = \mathcal{U}'_{\text{min}}$ is the energy minimum so $\mathcal{U}' \geq \mathcal{U}'_x$ and the distribution is asymmetric to the right. For a *negative* Gamma distribution, $\theta < 0$, $\mathcal{U}'_x = \mathcal{U}'_{\text{max}}$ is the energy maximum so $\mathcal{U}' \leq \mathcal{U}'_x$ and the distribution is asymmetric to the left. Only a positive Gamma distribution is physically completely correct (because every system must have an overall energy minimum); a negative Gamma distribution must be regarded as a (good) approximation to a more complex distribution.⁹ The moment generating function is

$$G_{\mathcal{U}'}^{\text{ref}}(t) \equiv \langle e^{t\mathcal{U}'} \rangle_{\text{ref}} = e^{t\mathcal{U}'_x} \left(\frac{\theta}{\theta - t} \right)^a \quad (17)$$

The free energy is via eqs 1 and 4 given by $A^*(T) = -kT \ln G_{\mathcal{U}'}^{\text{ref}}(-\beta)$. Differentiating the resulting expression in T and equating the expressions of $U^*(T)$, $C_V^*(T)$, and $\partial C_V^*(T)/\partial T$ at an arbitrary temperature T_0 to the corresponding thermodynamic values U_0^* , C_{V0}^* , and $\partial C_{V0}^*/\partial T$ (denoted by the zero subscript), one can solve the parameters \mathcal{U}'_x , a and θ in terms of U_0^* , C_{V0}^* , and $\partial C_{V0}^*/\partial T$. We define, moreover, $\theta = \beta_0(1 - \delta_0)/\delta_0$ with $\beta_0 = 1/kT_0$, and $U_{\Gamma 0}^*$ and $C_{V\Gamma 0}^* = ka\delta_0^2$, the excess energy and heat capacity in the Gamma region. In this case, where a single Gamma state is being used, the thermodynamic properties are identical to those of the average Gamma region (denoted by a subscript Γ): e.g., $U_{\Gamma 0}^* = U_0^*$, $C_{V\Gamma 0}^* = C_{V0}^*$, and $\partial C_{V\Gamma 0}^*/\partial T = \partial C_{V0}^*/\partial T$. In this way the familiar expressions are obtained^{9,13}

$$A^*(T) = A_{\Gamma}^*(T) = U_{\Gamma 0}^* - \frac{T_0 C_{V\Gamma 0}^*}{\delta_0} - \frac{T C_{V\Gamma 0}^*}{\delta_0^2} \ln(1 - \delta) \quad (18)$$

$$U^*(T) = U_{\Gamma}^*(T) = U_{\Gamma 0}^* + (T - T_0) C_{V\Gamma 0}^* \left(\frac{\delta}{\delta_0} \right) \quad (19)$$

$$C_V^*(T) = C_{V\Gamma}^*(T) = C_{V\Gamma 0}^* \left(\frac{\delta}{\delta_0} \right)^2 \quad (20)$$

$$S^*(T) = S_{\Gamma}^*(T) = \frac{C_{V\Gamma 0}^*}{\delta_0^2} [\delta + \ln(1 - \delta)] \quad (21)$$

$$\delta(T) = \frac{T_0 \delta_0}{T(1 - \delta_0) + T_0 \delta_0} \quad (22)$$

In these equations, as usual,

$$\delta_0 = \frac{T_0 \frac{\partial C_{V\Gamma 0}^*}{\partial T}}{2C_{V\Gamma 0}^*} + 1 = \frac{M_{3,0}[\mathcal{U}']_{\Gamma}}{2kT_0 M_{2,0}[\mathcal{U}']_{\Gamma}} \quad (23)$$

is a measure of the skewness of the energy distribution $\rho(\mathcal{U}')$ within the Gamma region at T_0 , defined by the ratio of the third and second central moments of \mathcal{U}' , i.e., $M_{3,0}[\mathcal{U}']$ and $M_{2,0}[\mathcal{U}']$, evaluated at T_0 . For $\delta_0 < 0$, $\delta_0 \rightarrow 0$, and $0 < \delta_0 < 1$, the distribution is left-skewed, symmetrical (Gaussian) or right-skewed, respectively. The model has three parameters (\mathcal{U}'_x , a , and θ of the reference state, or equivalently U_0^* , C_{V0}^* , and δ_0) that are related to three physical properties at the arbitrary reference temperature T_0 , e.g., U_0^* , C_{V0}^* , and $\partial C_{V0}^*/\partial T$.

A very simple set of mixing distributions arises if we assume that different regions of phase space are characterized by Gamma distributions with the same parameters a and θ , but with a different extreme energy value \mathcal{U}'_x . From eq 18 follows that in that case $\Delta A^*(T; \Delta \alpha) = \mathcal{U}'_x - \langle \mathcal{U}'_x \rangle_{\epsilon} = \mathcal{U}'_x - \mathcal{U}'_{x\Gamma} = \Delta \mathcal{U}'_x$, where we indicate the parameters of the average Gamma state by Γ . From eqs 9 and 10 it immediately follows that

$$A^*(T) = A_{\Gamma}^*(T) - kT \ln G_{\Delta \mathcal{U}'_x}^{\epsilon}(-\beta) \quad (24)$$

where $G_{\Delta \mathcal{U}'_x}^{\epsilon}(-\beta)$ is the moment generating function of the distribution of $\Delta \mathcal{U}'_x$, evaluated in $t = -\beta$, and $A_{\Gamma}^*(T)$ is given by eq 18. Any model parameter distribution must have a finite moment generating function for finite β . For \mathcal{U}'_x as a continuous variable, eq 24 directly yields a relation between the free energy A^* and the distribution $\rho_{\epsilon}(\Delta \mathcal{U}'_x)$:

$$A^*(T) = A_{\Gamma}^*(T) - kT \ln \int \rho_{\epsilon}(\Delta \mathcal{U}'_x) e^{-\beta \Delta \mathcal{U}'_x} d\Delta \mathcal{U}'_x \quad (25)$$

In case one assumes \mathcal{U}'_x to be a discrete variable, the simplest implementation (cf. Apol et al.²²) is to set $\mathcal{U}'_x = \mathcal{U}'_x + l \cdot \Delta \epsilon$ where $\Delta \epsilon$ is the energy gap between different values of \mathcal{U}'_x , and $l = 0, 1, \dots$. Note that, similar to the Gamma distribution, for a right-skewed distribution $\Delta \epsilon > 0$ with $\mathcal{U}'_x = \mathcal{U}'_{\text{MIN}}$, the absolute energy minimum, whereas for a left-skewed distribution $\Delta \epsilon < 0$ with $\mathcal{U}'_x = \mathcal{U}'_{\text{MAX}}$, the absolute energy maximum. In this way, the free energy is related to the (T -independent) probability p_l of a certain level l as

$$\begin{aligned} A^*(T) &= A_{\Gamma}^*(T) - kT \ln e^{\beta \Delta \epsilon \langle l \rangle_{\epsilon}} G_{\Gamma}^{\epsilon}(-\beta \Delta \epsilon) \\ &= A_{\Gamma}^*(T) - \langle l \rangle_{\epsilon} \Delta \epsilon - kT \ln \sum_{l=0}^{\infty} p_l e^{-\beta \Delta \epsilon l} \end{aligned} \quad (26)$$

3.1. Gaussian[\mathcal{U}'_x] Mixture of Gamma[\mathcal{U}'] States. The simplest possible continuous parameter distribution $\rho_{\epsilon}(\Delta \mathcal{U}'_x)$, although not completely physically allowed (because it is defined from $-\infty$ to $+\infty$), is the Gaussian distribution,^{20,23}

$$\rho_{\epsilon}(\Delta \mathcal{U}'_x) = \frac{1}{\sqrt{2\pi\sigma^2}} \exp\left\{ -\frac{(\Delta \mathcal{U}'_x)^2}{2\sigma^2} \right\} \quad (27)$$

Evaluating eq 25 yields with $\chi_0^* \equiv C_{V0}^* - C_{V\Gamma 0}^* = \sigma^2/kT_0^2$

$$\begin{aligned} A^*(T) &= A_{\Gamma}^*(T) - \frac{1}{2} T_0 \chi_0^* \left(\frac{T_0}{T} \right) \\ &= U_0^* - \frac{T_0 C_{V\Gamma 0}^*}{\delta_0} - \frac{T C_{V\Gamma 0}^*}{\delta_0^2} \ln(1 - \delta) + T_0 \chi_0^* \left(1 - \frac{T_0}{2T} \right) \end{aligned} \quad (28)$$

$$\begin{aligned} U^*(T) &= U_{\Gamma}^*(T) - T_0 \chi_0^* \left(\frac{T_0}{T} \right) \\ &= U_0^* + (T - T_0) C_{V\Gamma 0}^* \frac{\delta}{\delta_0} + T_0 \chi_0^* \left(1 - \frac{T_0}{T} \right) \end{aligned} \quad (29)$$

$$C_V^*(T) = C_{V\Gamma}^*(T) + \chi_0^* \left(\frac{T_0}{T} \right)^2 \quad (30)$$

$$S^*(T) = S_{\Gamma}^*(T) - \frac{1}{2} T_0 \chi_0^* \left(\frac{T_0}{T} \right) \quad (31)$$

where $A_{\Gamma}^*(T)$, $U_{\Gamma}^*(T)$, $C_{VT}^*(T)$, $S_{\Gamma}^*(T)$, and $\delta(T)$ are given by eqs 18–22. The model has four parameters (\mathcal{U}'_x , a , θ , and σ of the reference state, or equivalently U_0^* , C_{VT0}^* , δ_0 , and χ_0^*) that are related to four physical properties at the arbitrary reference temperature T_0 , e.g., U_0^* , C_{VT0}^* , $\partial C_{VT0}^*/\partial T$, and $\partial^2 C_{VT0}^*/\partial T^2$. χ_0^* is a measure of the variance of \mathcal{U}' at T_0 due to the spread in \mathcal{U}'_x , i.e., σ^2 . The skewness of the distribution of the extreme energy \mathcal{U}'_x is, being a symmetric Gaussian, obviously zero. A measure of the skewness of the overall potential energy distribution $\rho(\mathcal{U}')$ at T_0 , defined analogous to δ_0 (eq 23), is given by

$$\Delta_0 \equiv \frac{M_{3,0}[\mathcal{U}']}{2kT_0 M_{2,0}[\mathcal{U}']} = \frac{T_0 \frac{\partial C_{VT0}^*}{\partial T}}{2C_{VT0}^*} + 1 = \delta_0 \left(\frac{C_{VT0}^*}{C_{VT0}^*} \right) \quad (32)$$

Just as for the single Gamma state, the heat capacity $C_V^*(T)$ is monotonically decreasing with temperature. This statistical state, which we can write symbolically as Gaussian[\mathcal{U}'_x] \times Gamma[\mathcal{U}'], must be regarded as an approximation to a physically correct state, such as the following.

3.2. Gamma[\mathcal{U}'_x] Mixture of Gamma[\mathcal{U}'] States. The first continuous model distribution for $\rho_e(\Delta \mathcal{U}'_x)$ that can be completely physically allowed is the Gamma distribution,^{20,23}

$$\rho_e(\Delta \mathcal{U}'_x) = \frac{|\tau| \tau^{b-1}}{\Gamma(b)} \left(\Delta \mathcal{U}'_x + \frac{b}{\tau} \right)^{b-1} e^{-\tau(\Delta \mathcal{U}'_x + b/\tau)} \quad (33)$$

which has the same mathematical form as eq 16 but now expressed in terms of fluctuations around the average. Evaluating eq 25 and with a reparametrization similar to the single Gamma state [i.e., $\tau = \beta_0(1 - q_0)/q_0$ and $\chi_0^* \equiv C_{VT0}^* - C_{VT}^* = kbq_0^2$], one obtains

$$\begin{aligned} A^*(T) &= A_{\Gamma}^*(T) - \frac{T_0 \chi_0^*}{q_0(1 - q_0)} - \frac{T \chi_0^*}{q_0^2} \ln(1 - q) \\ &= U_0^* - \frac{T_0 C_{VT0}^*}{\delta_0} - \frac{T C_{VT0}^*}{\delta_0^2} \ln(1 - \delta) - \\ &\quad \frac{T_0 \chi_0^*}{q_0} - \frac{T \chi_0^*}{q_0^2} \ln(1 - q) \quad (34) \end{aligned}$$

$$\begin{aligned} U^*(T) &= U_{\Gamma}^*(T) - \frac{T_0 \chi_0^*}{1 - q_0} \left(\frac{q}{q_0} \right) \\ &= U_0^* + (T - T_0) C_{VT0}^* \left(\frac{\delta}{\delta_0} \right) + (T - T_0) \chi_0^* \left(\frac{q}{q_0} \right) \quad (35) \end{aligned}$$

$$C_V^*(T) = C_{VT}^*(T) + \chi_0^* \left(\frac{q}{q_0} \right)^2 \quad (36)$$

$$S^*(T) = S_{\Gamma}^*(T) + \frac{\chi_0^*}{q_0} [q + \ln(1 - q)] \quad (37)$$

$$q(T) = \frac{T_0 q_0}{T(1 - q_0) + T_0 q_0} \quad (38)$$

where $A_{\Gamma}^*(T)$, $U_{\Gamma}^*(T)$, $C_{VT}^*(T)$, $S_{\Gamma}^*(T)$, and $\delta(T)$ are given by eqs 18–22. The model has five parameters (\mathcal{U}'_x , a , θ , b , and τ of the reference state, or equivalently U_0^* , C_{VT0}^* , δ_0 , χ_0^* , and q_0) that are related to five physical properties at the arbitrary

reference temperature T_0 , e.g., U_0^* , C_{VT0}^* , $\partial C_{VT0}^*/\partial T$, $\partial^2 C_{VT0}^*/\partial T^2$, and $\partial^3 C_{VT0}^*/\partial T^3$. In this case,

$$q_0 = \frac{T_0 \frac{\partial \chi_0^*}{\partial T}}{2\chi_0^*} + 1 = \frac{M_{3,0}[\mathcal{U}'_x]}{2kT_0 M_{2,0}[\mathcal{U}'_x]} \quad (39)$$

is a measure of the skewness of the potential energy distribution $\rho(\mathcal{U}')$ at T_0 due to the distribution of \mathcal{U}'_x . Note that the central moments $M_{n,0}[\mathcal{U}'_x] = \langle (\mathcal{U}'_x - \langle \mathcal{U}'_x \rangle_0)^n \rangle_0$ of the extreme energy \mathcal{U}'_x are given in terms of ensemble averages; i.e., they are moments of the principle temperature-dependent probability distribution of finding the system in a state characterized by a specific value of \mathcal{U}'_x ; q_0 is in fact also the skewness of this distribution at T_0 .

The skewness of the overall potential energy distribution at T_0 (cf. eq 32) is given by the weighted average

$$\Delta_0 = \delta_0 \left(\frac{C_{VT0}^*}{C_{VT0}^*} \right) + q_0 \left(\frac{\chi_0^*}{C_{VT0}^*} \right) \quad (40)$$

When δ_0 and q_0 are both positive, the model can be considered completely physically allowed because in that case the energy is always larger than $\mathcal{U}'_{\text{MIN}}$. Just as for the single Gamma state and the Gaussian mixture of Gamma states, the heat capacity $C_V^*(T)$ is monotonically decreasing with temperature. The model can be written symbolically as Gamma[\mathcal{U}'_x] \times Gamma[\mathcal{U}'].

Note that the above expressions are (mathematically) symmetrical with respect to exchange of the parameters $\{C_{VT0}^*, \delta_0\}$ and $\{\chi_0^*, q_0\}$. One can, however, physically distinguish the two sets of parameters. Because for positive Gamma states ($\delta_0 > 0$) the effect of a distribution of \mathcal{U}'_x values should be most pronounced at low temperature (where \mathcal{U}' is relatively close to \mathcal{U}'_x), the parameters should be assigned in such a way that the contribution of the “average” Gamma state $C_{VT}^*(T)$ to the total heat capacity $C_V^*(T)$ increases with temperature. The assignment can also be facilitated by comparing the parameter sets of the Gaussian[\mathcal{U}'_x] \times Gamma[\mathcal{U}'] model with the Gamma[\mathcal{U}'_x] \times Gamma[\mathcal{U}'] model, because in the former case the parameters are mathematically distinct.

The Gamma[\mathcal{U}'_x] \times Gamma[\mathcal{U}'] expressions resemble those of the perturbed Gamma state that was used for the Lennard-Jones fluid over a very large temperature range (ref 15, eqs 46–49). One can convert the perturbed Gamma state parameters ΔU_{max} and γ to the Gamma mixture parameters χ_0^* and q_0 with the help of the equations $C_{VT0}^* - C_{VT}^* = \chi_0^* = 2\Delta U_{\text{max}} \gamma T_0 / (T_0 + \gamma)^3$ (cf. eq 52 of ref 15) and eq 39, where $\partial \chi_0^* / \partial T = \partial C_{VT0}^* / \partial T - \partial C_{VT}^* / \partial T = -2\Delta U_{\text{max}} \gamma (2T_0 - \gamma) / (T_0 + \gamma)^4$ (cf. eq 53 of ref 15). The result is

$$\begin{aligned} \chi_0^* &= \frac{2\Delta U_{\text{max}} \gamma T_0}{(T_0 + \gamma)^3} \\ q_0 &= \frac{3\gamma}{2(T_0 + \gamma)} \quad (41) \end{aligned}$$

3.3. Negative Binomial[\mathcal{U}'_x] Mixture of Gamma[\mathcal{U}'] States. In case one assumes that for some physical reason the extreme energy \mathcal{U}'_x can only assume discrete values separated by an energy gap $\Delta \epsilon$, one of the simplest discrete distributions of the T -independent level probability p_l is the negative binomial distribution,¹⁷

$$p_l = \binom{l+s-1}{l} (1-p)^l p^s \quad s > 0, 0 < p < 1 \quad (42)$$

for $l = 0, 1, \dots$. Evaluating eq 26 and defining the characteristic temperature $\Theta = \Delta\epsilon/k$, one obtains

$$\begin{aligned} A^*(T) &= A_{\Gamma}^*(T) - T_0 \chi_0^* \left(\frac{T_0}{\Theta} \right) \frac{\mathcal{N}_0^2}{p e^{-\Theta/T_0}} + \\ &\quad T_0 \chi_0^* \left(\frac{T_0}{\Theta} \right)^2 \frac{\mathcal{N}_0^2}{(1-p)e^{-\Theta/T_0}} \ln \left(\frac{\mathcal{N}}{p} \right) \\ &= U_0^* - \frac{T_0 C_{V\Gamma 0}^*}{\delta_0} - \frac{T C_{V\Gamma 0}^*}{\delta_0^2} \ln(1-\delta) - \\ &\quad T_0 \chi_0^* \left(\frac{T_0}{\Theta} \right) \mathcal{N}_0 + T_0 \chi_0^* \left(\frac{T_0}{\Theta} \right)^2 \frac{\mathcal{N}_0^2}{(1-p)e^{-\Theta/T_0}} \ln \left(\frac{\mathcal{N}}{p} \right) \quad (43) \end{aligned}$$

$$\begin{aligned} U^*(T) &= U_{\Gamma}^*(T) - T_0 \chi_0^* \left(\frac{T_0}{\Theta} \right) \frac{\mathcal{N}_0^2}{p e^{-\Theta/T_0}} \times \frac{1 - e^{-\Theta/T}}{\mathcal{N}} \\ &= U_0^* + (T - T_0) C_{V\Gamma 0}^* \frac{\delta}{\delta_0} + \\ &\quad T_0 \chi_0^* \left(\frac{T_0}{\Theta} \right) \frac{\mathcal{N}_0^2}{e^{-\Theta/T_0}} \left(\frac{e^{-\Theta/T}}{\mathcal{N}} - \frac{e^{-\Theta/T_0}}{\mathcal{N}_0} \right) \quad (44) \end{aligned}$$

$$C_{V\Gamma}^*(T) = C_{V\Gamma}^*(T) + \chi_0^* \left(\frac{T_0}{T} \right)^2 \left(\frac{\mathcal{N}_0}{\mathcal{N}} \right)^2 e^{-\Theta(1/T-1/T_0)} \quad (45)$$

$$\begin{aligned} S^*(T) &= S_{\Gamma}^*(T) - \chi_0^* \left(\frac{T_0}{T\Theta} \right) \frac{\mathcal{N}_0^2}{\mathcal{N}} e^{-\Theta(1/T-1/T_0)} - \\ &\quad \chi_0^* \left(\frac{T_0}{\Theta} \right)^2 \frac{\mathcal{N}_0^2}{(1-p)e^{-\Theta/T_0}} \ln \left(\frac{\mathcal{N}}{p} \right) \quad (46) \end{aligned}$$

where $A_{\Gamma}^*(T)$, $U_{\Gamma}^*(T)$, $C_{V\Gamma}^*(T)$, $S_{\Gamma}^*(T)$, and $\delta(T)$ are given by eqs 18–22 and where $\mathcal{N} = 1 - (1-p)e^{-\Theta/T}$ and $\mathcal{N}_0 = 1 - (1-p)e^{-\Theta/T_0}$. In these expressions we also used $s = (\chi_0^*/k)(T_0/\Theta)^2 \mathcal{N}_0^2 / [(1-p)e^{-\Theta/T_0}]$ and $\chi_0^* = C_{V0}^* - C_{V\Gamma 0}^*$. The model has five parameters (\mathcal{Z}'_x , a , θ , s , and $\Delta\epsilon$ of the reference state, or equivalently U_0^* , $C_{V\Gamma 0}^*$, δ_0 , χ_0^* , and Θ) that are related to five physical properties at the arbitrary reference temperature T_0 , e.g., U_0^* , C_{V0}^* , $\partial C_{V0}^*/\partial T$, $\partial^2 C_{V0}^*/\partial T^2$, and $\partial^3 C_{V0}^*/\partial T^3$. A measure of the skewness of the potential energy distribution at T_0 due to the distribution of \mathcal{Z}'_x (cf. eq 39) is given by

$$k_0 = \frac{1}{2} \left(\frac{\Theta}{T_0} \right) \left(\frac{1 + (1-p)e^{-\Theta/T_0}}{1 - (1-p)e^{-\Theta/T_0}} \right) \quad (47)$$

and the total skewness of the overall potential energy distribution at T_0 (cf. eq 32) is the weighted average

$$\Delta_0 = \delta_0 \left(\frac{C_{V\Gamma 0}^*}{C_{V0}^*} \right) + k_0 \left(\frac{\chi_0^*}{C_{V0}^*} \right) \quad (48)$$

The thermal behavior of the heat capacity C_V^* is a combination of the “classical” monotonic decrease with temperature (like the Gamma state) with superimposed an initial increase followed by a decrease to zero of the “quantum” contribution (like the

heat capacity of solids²²). The statistical state can be symbolically written as $\text{NBin}[\mathcal{Z}'_x] \times \text{Gamma}[\mathcal{Z}']$.

4. Results and Discussion

In this section the new statistical states, especially the $\text{Gamma}[\mathcal{Z}'_x] \times \text{Gamma}[\mathcal{Z}']$ state, will be applied to several systems consisting of small molecules without semiclassical intramolecular degrees of freedom, for which the reduced or residual properties X^* (with respect to the ideal gas) are identical⁹ to the ideal reduced properties X' . Note that the ideal reduced energy (U^*) and temperature derivatives such as the heat capacity (C_V^*) are also identical to the confined ideal reduced properties (U^* and C_V^*). As indicated in the previous sections, for all models a limited set of input data at one temperature T_0 is sufficient, e.g., the “potential” energy U_0^* and some temperature derivatives such as C_{V0}^* , $\partial C_{V0}^*/\partial T$, In the following applications, the experimental value of U_0^* is being used, and the remaining two to four parameters of the model at hand ($C_{V\Gamma 0}^*$, δ_0 , ...) are obtained by fitting the $U^*(T)$ expression to experimental data within some specified temperature interval. This is conceptually equivalent to fitting a polynomial to selected $U^*(T)$ data around T_0 and evaluating the required energy derivatives C_{V0}^* , ..., $\partial^n C_{V0}^*/\partial T^n$ to obtain all parameters of the model. Previously^{9,16,18} we have shown that the QGE Gamma model, eq 19, can extrapolate thermodynamic functions over large temperature ranges only on the basis of information close to T_0 . In this study, we would like to show, in general, the applicability of the $\text{Gamma}[\mathcal{Z}'_x] \times \text{Gamma}[\mathcal{Z}']$ model for various systems and conditions. Therefore, to obtain the most accurate parameters, we used a fitting procedure within a specified temperature window.

4.1. Hard Core Yukawa Fluid. The first system that was studied is the hard core Yukawa fluid, with an interaction potential of the form

$$u(r) = \begin{cases} \infty & r < \sigma \\ -\epsilon \frac{e^{-z(r-\sigma)/\sigma}}{r/\sigma} & r \geq \sigma \end{cases} \quad (49)$$

where the parameter z determines the interaction range. For a value $z = 1.8$ the system is claimed to give results similar to the Lennard-Jones system.²⁴ The potential is, e.g., used as a model potential for charged colloids with screened Coulombic interactions. Duh and Mier-y-Terán²⁴ have formulated an explicit EOS for this system by means of an analytical continuation and summation of the first five terms of the high-temperature free energy expansion given by Henderson and co-workers²⁵ within the mean spherical approximation (MSA). At various state points, the EOS very accurately reproduces the exact MSA results of Henderson et al.,²⁶ and for various values of z , the EOS yields coexistence lines that compare well with results from Gibbs Ensemble Monte Carlo simulations, except very close to the critical point. According to the EOS, for $z = 1.8$ the critical point (in reduced units) is $T_c \cong 1.24$ and $\rho_{Nc} \cong 0.319$. Using the EOS, $U^*(T)$ data at 22 isochores with density $\rho_N = 0.01, 0.03, 0.05(0.05)1.0$ were generated from the coexistence line up to $T = 6$ (i.e., $\sim 5T_c$), and the reference temperature was set to $T_0 = 1.5$ at all isochores.

For this large temperature interval, a single Gamma state (eq 19) provides a very accurate description of the data from the coexistence line on. Parameters are shown in Figure 2. Extension of the temperature range up to $T = 20$ ($\sim 16T_c$) and $T = 50$ ($\sim 40T_c$) yields exactly the same parameters with the same accuracy, suggesting that the Gamma distribution is a very good

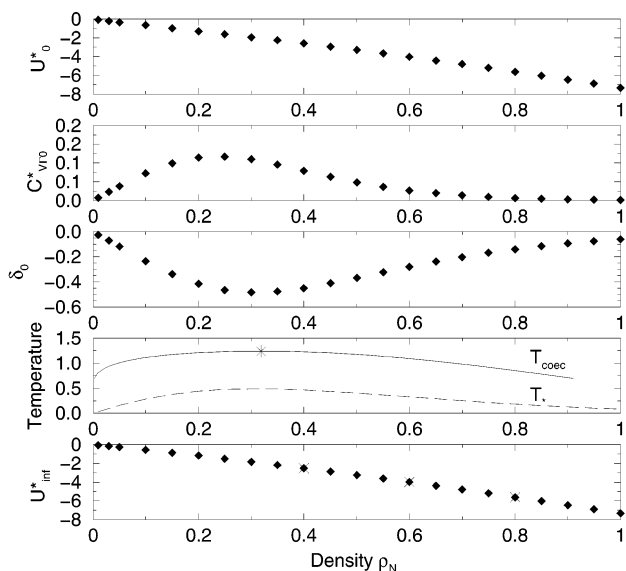


Figure 2. Parameters U_0^* , C_{VT0}^* and δ_0 of the Gamma[\mathcal{U}'] state, eq 19, for the hard core Yukawa fluid at various densities for $T \leq 6$ with $T_0 = 1.5$ (◆). Also shown are the coexistence line T_{coex} (—), the singular temperature T_* of the negative Gamma state (---), and the infinite temperature potential energy of the Gamma state, U_{inf}^* (◆), together with values of Henderson et al. within the MSA²⁶ (×). The critical point is indicated by *.

approximation to the real potential energy distribution within the MSA. In fact, it was impossible to obtain reliable parameters for the Gaussian[\mathcal{U}'_x]×Gamma[\mathcal{U}'] or Gamma[\mathcal{U}'_x]×Gamma[\mathcal{U}'] state models (eqs 29 and 35). Obviously, the EOS (and data used) are based on the MSA, but an analysis based on fluid data from Monte Carlo simulations, for example, would probably yield reasonably similar results.

Interestingly, at all densities the distribution is left-skewed ($\delta_0 < 0$) due to the attractive interactions and the lack of continuous repulsive forces. The distribution is most asymmetric around the critical density. For negative Gamma states, as encountered here, there is a singular temperature $T_* = -T_0\delta_0/(1 - \delta_0) > 0$ for $\delta_0 < 0$ at which the thermodynamics is undefined.⁹ In Figure 2 this temperature is shown, together with the coexistence line T_{coex} . At all densities, T_* is well below T_{coex} . Interestingly, at $\rho_N \rightarrow 0$ the singular temperature goes exactly to zero, meaning that there is no singularity in the ideal gas limit, as should be. Finally, also the infinite temperature energy limit $U_{\text{inf}}^* = \lim_{T \rightarrow \infty} U^*(T) = U_0^* + T_0 C_{VT0}^*/(1 - \delta_0)$ (see ref 9) is shown in Figure 2, along with exact MSA results from Henderson.²⁶ Both sets match extremely well, again showing that a single Gamma state is a perfect description of the hard core Yukawa fluid within the MSA.

4.2. Lennard-Jones Fluid. We also reanalyzed $U^*(T)$ data of the truncated and shifted Lennard-Jones (LJ) system,¹⁵ for 10 isochores with density (in reduced LJ units) $\rho_N = 0.1(0.1)1.0$ and temperatures from the coexistence line up to $T = 20$. The data are identical to those used to parametrize a full EOS for the LJ system based on a perturbed Gamma state.¹⁵ The critical point of the truncated and shifted LJ system using *NVT* simulations (without long-range and shift corrections) is $T_c \cong 1.29$ and $\rho_{Nc} \cong 0.348$ (ref 15). The reference temperature was set to $T_0 = 2.0$.

For such a large temperature interval ($\sim 15T_c$) a single Gamma state (eq 19) is not accurate enough. However, for a more restricted temperature range ($T \leq 6.0 \sim 4T_c$) a single Gamma state is accurate for “liquid” isochores ($\rho_N \geq 0.6$). The Gamma-[\mathcal{U}'_x]×Gamma[\mathcal{U}'] state model (eq 35), however, perfectly

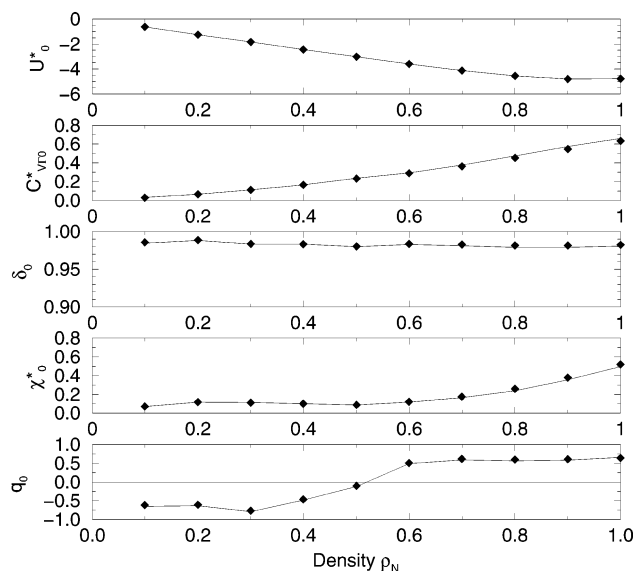


Figure 3. Parameters of the Gamma[\mathcal{U}'_x]×Gamma[\mathcal{U}'] state for the Lennard-Jones fluid at various densities with $T_0 = 2.0$: (1) direct use of eq 35 (◆); (2) conversion of perturbed Gamma state parameters (ref 15) using eq 40 (—).

describes the simulation data over the entire temperature range. Parameter values for the 10 isochores, obtained by fitting eq 35 to the $U^*(T)$ simulation data, are given in Figure 3. Also the parameter values of the perturbed Gamma state expression from ref 15, converted to Gamma[\mathcal{U}'_x]×Gamma[\mathcal{U}'] state parameters via eq 41, are shown in the same figure. There is a perfect agreement between the two sets of parameter values, indicating that the perturbed Gamma state is in fact just a good approximation to the Gamma[\mathcal{U}'_x]×Gamma[\mathcal{U}'] state, and the “average” Gamma state of the Gamma[\mathcal{U}'_x]×Gamma[\mathcal{U}'] model coincides with the Gamma state region of the perturbed Gamma state model, cf. the white region in Figure 1c,d. As explained in section 3.2, the parameters were assigned in such a way that the contribution of the average Gamma state to the heat capacity is increasing with temperature. The asymmetry of the basic Gamma distributions of the mixture is more or less density independent and very positive ($\delta_0 \sim 0.98$), and the Gamma heat capacity C_{VT0}^* increases monotonically with density. The distribution of \mathcal{U}'_x is left-skewed ($q_0 < 0$) for densities below ~ 0.5 , and right-skewed for larger densities. In this way also the overall potential energy distribution changes from left-skewed at low density ($\Delta_0 < 0$, cf. eq 40) to right-skewed ($\Delta_0 > 0$) at high density, due to a changing balance between attractive and repulsive interactions. Similar behavior has been observed for water and methane¹⁴ and in the previous analysis of the LJ fluid;¹⁵ see also section 4.8. From an analysis of the relative contribution of $C_{VT}^*(T)$ to the total heat capacity $C_V^*(T)$ it follows that the mixing contribution is especially important for gas densities at relatively low temperature.

4.3. Argon. Data of the residual energy $U^r = U^*$ of argon were obtained from the equation of state of Tegeler, Span, and Wagner⁵ at 25 isochores (0.001, 0.005, 0.01, 0.05, 0.1, 0.25, 0.5, 0.75, 1, 1.5, 2, 2.5(2.5)35 mol/dm³) from the coexistence line to 700 K. The critical point is located at $T_c = 150.7$ K and $\rho_{Nc} = 13.41$ mol/dm³. The reference temperature was set to $T_0 = 180$ K.

A single Gamma state model (eq 19) for temperatures up to 700 K ($\sim 5T_c$) is not accurate enough, except at high densities ($\rho_N \geq 22.5$ mol/dm³), just like for the LJ system. For a more restricted range up to 300 K ($\sim 2T_c$), a single Gamma state

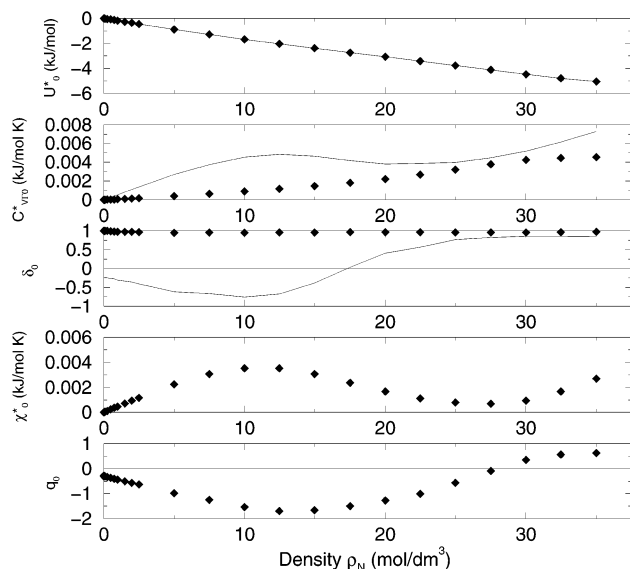


Figure 4. Parameters of the Gamma[\mathcal{U}'_x]×Gamma[\mathcal{U}'] state, eq 35, for argon at various densities for $T \leq 700$ K (◆) and of the single Gamma state, eq 19, for $T \leq 300$ K (◊) with $T_0 = 180$ K.

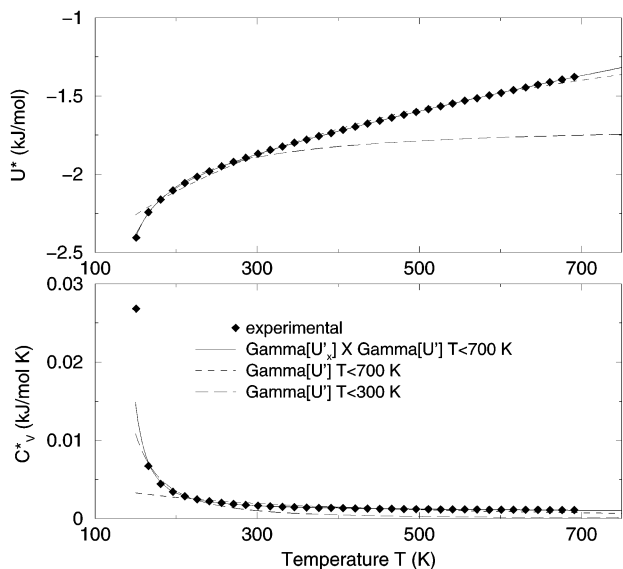


Figure 5. Potential energy U^* and heat capacity C^*_v of argon vs temperature at the critical isochore 13.41 mol/dm^3 and Gamma[\mathcal{U}'] and Gamma[\mathcal{U}'_x]×Gamma[\mathcal{U}'] state models (eqs 19 and 35).

provides an accurate description almost from the coexistence line for typical “gas” ($\rho_N \lesssim 7.5 \text{ mol/dm}^3$) and “liquid” densities ($\rho_N \gtrsim 22.5 \text{ mol/dm}^3$). For intermediate densities a single Gamma state still provides a fair description; see also Figure 5. The corresponding parameters are shown in Figure 4. A Gamma[\mathcal{U}'_x]×Gamma[\mathcal{U}'] model (eq 35), however, provides an excellent description of the system over the entire temperature range, including the vicinity of the critical point. In Figure 4 the corresponding parameters are shown as a function of density. There is a clear similarity between these parameters and the parameters of the LJ fluid (Figure 3). Also in this case the Gamma distributions of the mixture are very right-skewed ($\delta_0 \sim 0.96\text{--}0.98$). In contrast to the decrease of C^*_{v0} of the single Gamma state model between 12.5 and 20 mol/dm^3 , C^*_{vT0} in the Gamma[\mathcal{U}'_x]×Gamma[\mathcal{U}'] model increases monotonically; this is compensated by the behavior of χ^*_0 , as $C^*_{v0} = C^*_{vT0} + \chi^*_0$. Figure 5 shows the critical isochore ($\rho_N = 13.41 \text{ mol/dm}^3$) with the single Gamma states ($T \leq 300$ K, $T \leq 700$

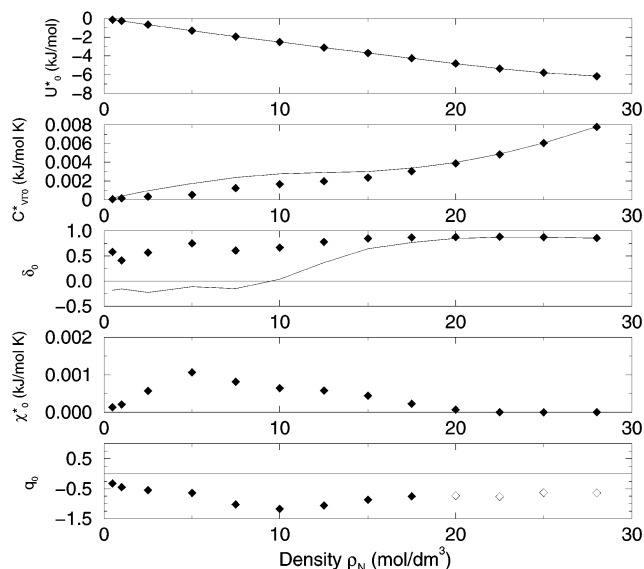


Figure 6. Parameters of the Gamma[\mathcal{U}'_x]×Gamma[\mathcal{U}'] state, eq 35, for methane at various densities (◆) and of the single Gamma state, eq 19 (◊) with $T_0 = 301$ K. Ill-defined parameter values of the Gamma mixture model (see text) are indicated by ◊.

K) and the Gamma[\mathcal{U}'_x]×Gamma[\mathcal{U}'] model that is able to describe the behavior of $U^*(T)$ and $C^*_v(T)$ over the whole temperature range. Obviously, the Gamma mixture model cannot describe the true divergence of C^*_v at the critical point. However, part of the steep increase of C^*_v that is also present in general close to the coexistence line at other noncritical isochores, can be accurately described by the model. Note that the parameters are very smooth functions of density, even around the critical point. A detailed description of the critical point and its close vicinity would require additional theory, e.g., renormalization group theory with a “crossover” equation of state.^{27–29}

4.4. Methane. Data of the residual energy $U^r = U^*$ of methane (CH_4) at 13 selected isochores ($0.5, 1.0, 2.5(2.5)25.0$ and 28.0 mol/dm^3) were obtained from the NIST Chemistry Webbook,³⁰ on the basis of the equation of state of Setzmann and Wagner⁶ from the coexistence line up to 621 K. The critical parameters are $T_c = 190.6$ K and $\rho_{Nc} = 10.14 \text{ mol/dm}^3$. The reference temperature was set to $T_0 = 301$ K.

Just as for the LJ system and argon, for this temperature range (up to $\sim 3T_c$), a single Gamma state (eq 19) accurately describes “gas” isochores ($\rho_N \leq 5 \text{ mol/dm}^3$) and “liquid” isochores ($\rho_N \geq 17.5 \text{ mol/dm}^3$). The corresponding parameters are given in Figure 6, and the behavior in density is very similar to argon. The Gamma[\mathcal{U}'_x]×Gamma[\mathcal{U}'] model (eq 35), however, perfectly describes the data over the entire temperature range, including the coexistence line and the vicinity of the critical point for all isochores. Parameters are shown in Figure 6, and also these parameters are very similar to those of the LJ system and argon (Figures 3 and 4): the Gamma energy distributions of the mixture are rather right-skewed ($\delta_0 \sim 0.6\text{--}0.85$) but less asymmetric than for the LJ system and argon. At $\sim 20 \text{ mol/dm}^3$ and above, the C^*_{vT0} values of a single Gamma state and the Gamma[\mathcal{U}'_x]×Gamma[\mathcal{U}'] model virtually coincide, indicating that the influence of the “mixture” is negligible ($\chi^*_0 \approx 0$), so the mixture model reduces to the single “average” Gamma model. Hence the values of q_0 are numerically rather ill-defined in this region; i.e., the model is rather insensitive to the precise value of q_0 . In the figure this is indicated by open symbols. Up to $\sim 20 \text{ mol/dm}^3$, the behavior of q_0 is (within the noise) smooth

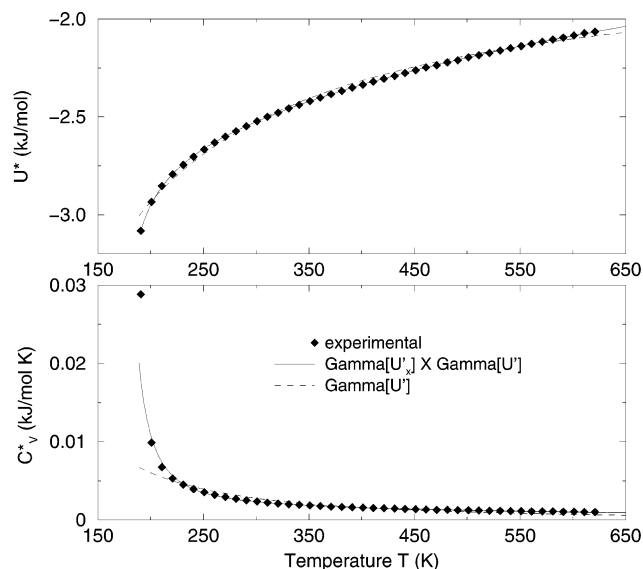


Figure 7. Potential energy U^* and heat capacity C_v^* of methane vs temperature at the near-critical isochore 10 mol/dm³ and Gamma[U'] and Gamma[U'] \times Gamma[U'] state models (eqs 19 and 35).

and similar to the previous systems. In Figure 7, the data of $U^*(T)$ and $C_v^*(T)$ for the near-critical isochore $\rho_N = 10$ mol/dm³ are shown, together with the single Gamma state model and Gamma[U'] \times Gamma[U'] model. The latter model perfectly reproduces the potential energy and heat capacity, including a very large part of the divergence of C_v^* at the critical point, even though the parameters such as for argon are all very smoothly depending on density, even around the critical point. Note that the behavior of $C_v^*(T)$ at intermediate densities (including the critical one) is very regular, i.e., smoothly decreasing with temperature, in contrast to the behavior that was observed using older experimental data.¹⁴

4.5. Ammonia. Data of the residual energy $U^r = U^*$ of ammonia (NH₃) at 23 isochores (0.01, 0.1, 0.25, 0.5, 1.0, 1.5, 2.5(2.5)42.5 mol/dm³) were obtained from the NIST Chemistry Webbook,³⁰ on the basis of the equation of state of Tillner-Roth, Harms-Watzenberg, and Baehr³¹ from the coexistence line up to 700 K. The critical point is $T_c = 405.4$ K and $\rho_{Nc} = 13.21$ mol/dm³. The reference temperature was set to $T_0 = 430$ K.

For the given temperature range ($\sim 1.7T_c$), a single Gamma state is actually very accurate for typical “gas” ($\rho_N \leq 4$ mol/dm³) and “liquid” densities ($\rho_N \geq 20$ mol/dm³). For intermediate densities the accuracy is good, but only close to the coexistence line, there is a small temperature window with some deviations. Parameters are shown in Figure 8.

The Gamma[U'] \times Gamma[U'] model (eq 35) significantly improves the accuracy at those intermediate densities and provides an excellent description from the coexistence line up to 700 K at all isochores. The parameters are shown in Figure 8. There are two density regions that show some special features: at high density ($\rho_N \geq 30$ mol/dm³) the parameters δ_0 and q_0 are virtually equal, meaning that in fact the mixture model reduces to a single (positive) Gamma state. In the figure clearly the values of δ_0 of the single Gamma state coincide at high density with the δ_0 values of the Gamma mixture model, and the values of χ_0^* ($=C_{VT0}^* - C_{VT}^*$) and q_0 are therefore numerically rather ill-defined. In the figure they are indicated by open symbols. The other region is at very low density ($\rho_N < 2.5$ mol/dm³), where the “average” Gamma state parameters C_{VT0}^* and especially δ_0 are rather ill-defined: for a broad range of C_{VT0}^* and δ_0 values the model provides virtually the same behavior.

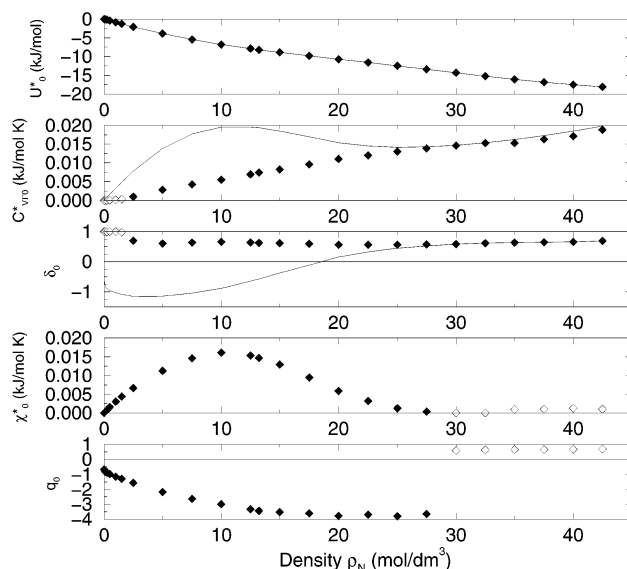


Figure 8. Parameters of the Gamma[U'] \times Gamma[U'] state, eq 35, for ammonia at various densities (◆) and of the single Gamma state, eq 19 (◇) with $T_0 = 430$ K. Ill-defined parameter values of the Gamma mixture model are indicated by ◇; see text.

From the analysis of the relative contribution of $C_{VT}^*(T)$ to the total heat capacity $C_v^*(T)$ it follows that at low density the heat capacity is completely determined by the parameters χ_0^* and q_0 . Probably the temperature range is too small to define in a stable way the “average” Gamma state that should dominate at high temperature. Hence in Figure 8 the parameters C_{VT0}^* and δ_0 are in this region also indicated by open symbols. At all isochores, the energy distributions of the mixture are rather right-skewed ($\delta_0 \sim 0.6-0.7$), but significantly less asymmetric than for the LJ system and argon.

4.6. Water. Data of the residual energy $U^r = U^*$ of water at 34 isochores (0.005, 0.01, 0.05, 0.1, 0.25, 0.5, 0.75, 1.0, 1.5, 2.0, 2.5(2.5)60.0 mol/dm³) were obtained from the EOS by Saul and Wagner⁸ from the coexistence line up to 1273 K ($\sim 2T_c$). The critical point is located at $T_c = 647.1$ K and $\rho_{Nc} = 17.87$ mol/dm³. The reference temperature was set to $T_0 = 673$ K.

In accordance with previous results,^{9,13,14,18} for all isochores already a single Gamma state model (eq 19) very accurately describes the data within this temperature range, except for a small temperature window of at most ~ 5 K located at the coexistence line for $2.0 \leq \rho_N \leq 25$ mol/dm³. Parameters are shown in Figure 9. For densities below 32 mol/dm³, the potential energy distribution is left-skewed ($\delta_0 < 0$) due to predominant attractive interactions, above that density the distribution is right-skewed ($\delta_0 > 0$).

Experimental data over an even larger temperature range are difficult to obtain; therefore we used the Saul and Wagner EOS to generate data up to 2073 K ($\sim 3T_c$). Although the EOS has been parametrized up to 1273 K, its description of shock-wave experiments⁸ suggests that it might be used to extrapolate over a larger temperature range. Again, a single Gamma state model perfectly describes the data, with parameters that are almost identical to the parameters up to 1273 K (see Figure 9). This confirms that a single Gamma distribution is an excellent model for the potential energy distribution of water.

Because the distribution is so close to a single Gamma distribution, it is somewhat difficult to obtain reliable parameters for mixing distributions, such as a Gaussian[U'] \times Gamma[U'] (eq 29) or Gamma[U'] \times Gamma[U'] model (eq 35). In fact, a Gaussian[U'] \times Gamma[U'] model does not improve

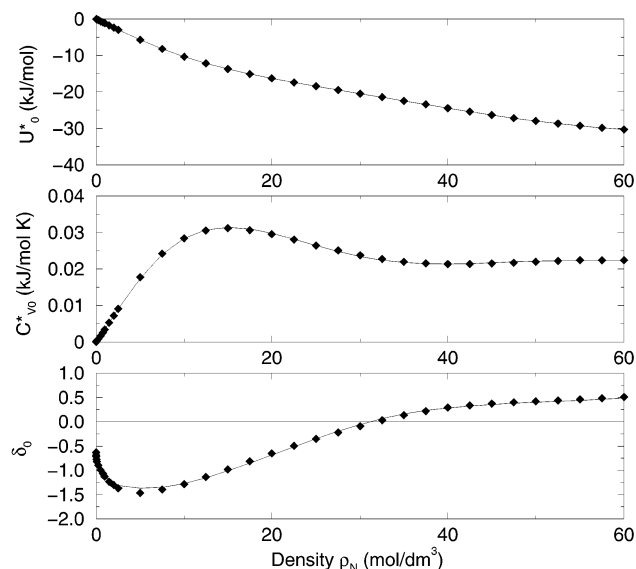


Figure 9. Parameters of the single Gamma[\mathcal{U}'] state, eq 19, for water at various densities with $T_0 = 673$ K: (1) based on data within the range $T \leq 1273$ K (\blacklozenge); (2) based on data within the range $T \leq 2073$ K (\circ).

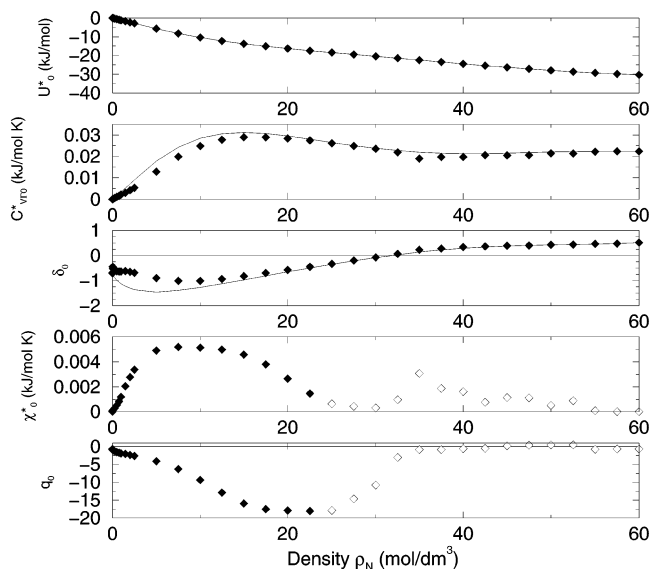


Figure 10. Parameters of the Gamma[\mathcal{U}'_1] \times Gamma[\mathcal{U}'] state, eq 35, for water at various densities for $T \leq 1273$ K (\blacklozenge) and of the single Gamma state, eq 19, for $T \leq 673$ K (\circ) with $T_0 = 673$ K. Ill-defined parameter values (see text) are indicated by \diamond .

the accuracy close to the coexistence line. On the other hand, the Gamma[\mathcal{U}'_1] \times Gamma[\mathcal{U}'] model is able to describe the residual energy up to the coexistence line, including the vicinity of the critical point. Parameters are shown in Figure 10, together with the single Gamma state parameters. In contrast to the previous systems, $C_{VT_0}^*$ is not monotonically increasing with density but behaves rather similar to C_{V0}^* of the single Gamma state, indicating that a single Gamma state is already a very accurate model. It follows from the figure, as well as from evaluating the relative contribution of the average Gamma state $C_{VT}^*(T)$ to the total heat capacity $C_V^*(T)$, that the effect of the mixing distribution is most pronounced at “gas” densities below the critical isochore. For typical “liquid” isochores ($\rho_N \geq 25$ mol/dm³) the average Gamma state is by far the dominant part (more than 95–99% contribution to the heat capacity; note that in this region the $C_{VT_0}^*$ of the single Gamma and Gamma mixture models virtually coincide). The parameters χ_0^* and q_0

TABLE 1: Molecular Dynamics Results of SPC/E Water as a Function of Temperature at 55.509 mol/dm³

T (K)	Δt (fs)	t_{sim} (ps)	U^* (kJ/mol)	C_V^* [kJ/(mol K)]
250	3.0	12000	-49.5199(22)	0.0628
275	2.0	12000	-47.9928(16)	0.0750
300	2.0	9000	-46.4680(14)	0.0545
350	2.0	6500	-43.7998(14)	0.0449
400	1.0	5000	-41.6348(14)	0.0404
500	1.0	3000	-37.9149(17)	0.0315
600	1.0	3000	-34.9234(17)	0.0259
800	0.5	1500	-30.2647(24)	0.0198
1000	0.5	1500	-26.6189(24)	0.0162
1200	0.5	1500	-23.5697(24)	0.0138
1600	0.25	1400	-18.5772(26)	0.0111
2000	0.25	1400	-14.4875(27)	0.0093
2400	0.125	650	-10.9801(43)	0.0082
2800	0.125	650	-7.8892(46)	0.0073

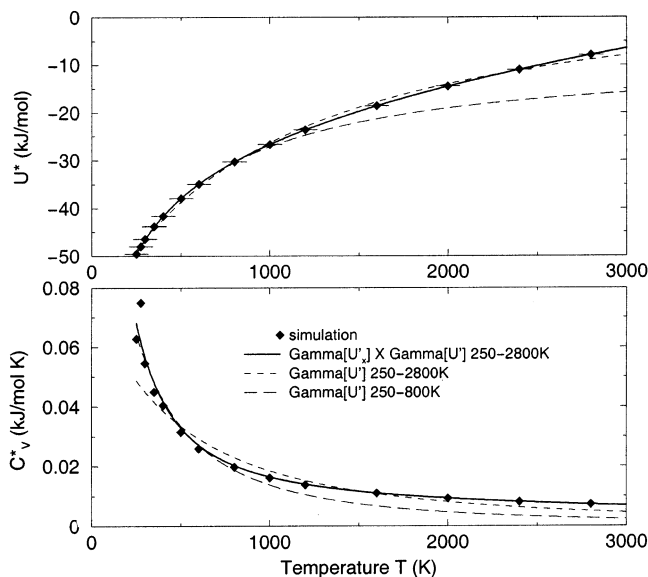
are therefore numerically less well defined, and hence the “irregularities” of these parameters in density are very likely not physically meaningful; in fact, there is a range of q_0 (and χ_0^*) values that give almost identical results. In the figure they are therefore indicated by open symbols. It is interesting to note that the density behavior of the parameters around the critical point is very smooth, as with the other systems. It is worth remarking that, similar to the case of methane, the irregular behavior of $C_V^*(T)$ that was observed in a previous analysis at high density^{9,14} must be attributed to artifacts of the older experimental data, very likely the mathematical shape of the function to correlate raw experimental measurements.

4.7. SPC/E Water. To investigate the behavior of water over a very large temperature interval in more detail, molecular dynamics simulations were performed with the extended simple point charge (SPC/E) water model³² at a liquid density of 55.509 mol/dm³ ($=1.0$ g/cm³) for temperatures between 250 and 2800 K. This model has been chosen because it reproduces in the best way, among the different (non)polarizable water models, various static and dynamic properties of water.^{33–35} Simulations were performed using the GROMACS 3.0 software package,^{36–38} with periodic boundary conditions, particle mesh Ewald summation^{39,40} (PME) with conducting boundary conditions for the long-range electrostatic interactions, and a leapfrog Verlet integration algorithm. The temperature was kept constant by a Berendsen thermostat⁴¹ with coupling time $\tau_T = \Delta t$ mimicking a Gaussian thermostat.^{42,43} Constraints were handled by SETTLE.⁴⁴ Each state point was equilibrated for 100 ps, and the total length of the production runs (t_{sim}) is given in Table 1, as well as the values of the time step Δt and average potential energy U^* . Error bars were determined by the block-average method.^{45–47} The heat capacity was calculated from fluctuations of the total potential energy.^{15,16}

A single Gamma state model was fitted to the $U^*(T)$ data over the entire temperature range, as well as in the low (250–800 K) and high-temperature range (1000–2800 K). Also the Gaussian and Gamma mixtures of Gamma states were used. Parameters are presented in Table 2, and some models are shown in Figure 11. Although a single Gamma state fitted over the complete temperature range gives a very reasonable description of the potential energy, some discrepancies in the heat capacity are visible. A Gamma state fitted at low temperature (250–800 K) provides locally a very accurate model, but extrapolations to 2800 K are less accurate. However, the Gaussian-[\mathcal{U}'_1] \times Gamma[\mathcal{U}'] and Gamma[\mathcal{U}'_1] \times Gamma[\mathcal{U}'] models provide an excellent description over the whole temperature range, including “metastable” states at low temperature. Interestingly, the parameters $C_{VT_0}^*$ and δ_0 of both the Gaussian and

TABLE 2: Various Statistical States of SPC/E Water and Experimental Water at 55.509 mol/dm³ with $T_0 = 300$ K

model	T range (K)	U_0^* (kJ/mol)	C_{VT0}^* [kJ/(mol K)]	δ_0	χ_0^* [kJ/(mol K)]	q_0
SPC/E						
Gamma[\mathcal{U}']	250–2800	−46.4680	0.0450	0.7613		
Gamma[\mathcal{U}'']	250–800	−46.4680	0.0554	0.5701		
Gamma[\mathcal{U}''']	1000–2800	−39.9160	0.0236	0.8989		
Gaussian[\mathcal{U}'_i]×Gamma[\mathcal{U}']	250–2800	−46.4680	0.0199	0.9049	0.0398	
Gamma[\mathcal{U}'_i]×Gamma[\mathcal{U}']	250–2800	−46.4680	0.0106	0.9621	0.0460	0.3697
Water						
Gamma[\mathcal{U}']	315–800	−41.3378	0.0461	0.6452		

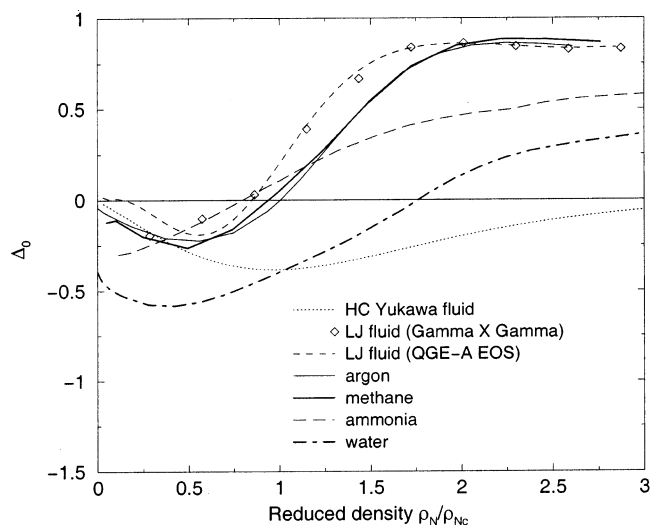
**Figure 11.** Potential energy U^* and heat capacity C_V^* of SPC/E water vs temperature at $\rho_N = 55.51$ mol/dm³: simulation data (\blacklozenge) and some QGE statistical states with $T_0 = 300$ K.

Gamma mixture models are very similar to the values of C_{VT0}^* and δ_0 of the single Gamma state model fitted at high temperature; see Table 2. This is also an indication that the assignment of the parameters $\{C_{VT0}^*, \delta_0\}$ and $\{\chi_0^*, q_0\}$ is physically the correct one. For comparison, in the table also parameter values are shown of a single Gamma state using $U^*(T)$ data of real water.⁸ The parameters are remarkably similar to those of SPC/E, taking into account the lowering of potential energy in SPC/E due to the “self-polarization” energy³² of 5.22 kJ/mol.

4.8. General Remarks. In Figure 12 we show the asymmetry of the potential energy distribution Δ_0 (eq 32) for all systems as a function of the scaled density ρ_N/ρ_{Nc} at a common reference temperature $T_0 = 1.5T_c$. The figure suggests several points for systems of small molecules:

(1) A system with only (continuous) attractive interactions (like the hard core Yukawa fluid) is characterized by a left-skewed potential energy distribution. The maximum skewness occurs very close to the critical point. With a further increase of density, the number of interactions per molecule also increases, and so using a form of the central limit theorem,²⁰ it is plausible that the distribution of the total potential energy, being the sum of all individual contributions, becomes more Gaussian, i.e., $\delta_0 \rightarrow 0$.

(2) (Continuous) repulsive interactions (present in all other systems) superimpose an extra effect on the previous density behavior of the skewness Δ_0 : with increasing density repulsions become more pronounced, resulting in a (very) asymmetric right-skewed distribution. This shifts the density of maximum left-skewness to values lower than the critical density.

**Figure 12.** Asymmetry Δ_0 of the potential energy distribution $\rho(\mathcal{U}')$ for various systems as a function of density at a common reference temperature $T_0/T_c = 1.5$.

(3) Roughly speaking, the polarity of the molecules simply shifts the Δ_0 curves upward or downward. The curves of very apolar systems (LJ fluid, argon, methane) are all very similar, as to be expected. For ammonia, and especially water, which are (very) polar, the long-range electrostatic interactions are at relatively low density ($\sim 0.5\rho_{Nc}$) very attractive and result in a distribution that is much more left-skewed than systems with only van der Waals interactions (LJ, argon, methane). At higher density, the long-range character of the Coulombic interactions results via the central limit theorem again in a more Gaussian like distribution. Indeed, at liquid density, the potential energy distribution of water is less asymmetric than that of ammonia, which in turn is less asymmetric than pure van der Waals systems. In this respect, water is a much “simpler” liquid than argon, as the energy distribution of the former is much more Gaussian and a single Gamma state is able to extrapolate over a much larger temperature range than in the case of argon. Moreover, within a temperature range of $\sim 2T_c$, in the case of water a single Gamma state can accurately describe the thermodynamic data at all isochores, whereas for argon a single Gamma state only provides an accurate model at low and high densities within the same temperature range. Interesting, it seems that the complexity of a system according to the “distribution point of view” is the opposite of the “molecular Hamiltonian point of view”.¹¹

Another interesting point is the fact that for typical liquid densities the Gamma distributions of the “mixtures” are all very right-skewed ($\delta_0 \sim 1$), especially for the LJ fluid, argon, and SPC/E water. This suggests that the potential energy “landscape” of these systems may be described as a collection of almost harmonic wells (for which δ_0 would be exactly unity^{13,16}). This also fits very well with the idea of a (potential) energy landscape of harmonic wells, as worked out for liquids and glasses by

Stillinger and Debenedetti^{48–50} and for biomacromolecules by Amadei et al.⁵¹ Interestingly, the potential energy wells of (experimental) water, ammonia, and methane are less harmonic ($\delta_0 \sim 0.5–0.85$) than those of the LJ fluid, argon, and the (simulated) SPC/E water model. Further research in this direction is in progress.

5. Conclusions

In this article a general derivation of multistate thermal models for fluid systems has been given, on the basis of a physical partitioning of the system's phase space into multiple regions. Within the framework of the quasi-Gaussian entropy (QGE) theory, the (residual) Helmholtz free energy is given by the moment generating function of the potential energy distribution. For the new multistate models, this distribution is a "mixture" of "simple" distributions, mixed according to some parameter distribution.

Some multistate models have been derived using a mixture of Gamma distributions for the potential energy \mathcal{U}' , each with a different value of the extreme energy \mathcal{U}'_x (i.e., potential energy minimum in most cases). They have been applied to and tested on several small molecules: the hard core Yukawa fluid, the Lennard-Jones (LJ) fluid, argon, methane, ammonia, water, and the SPC/E water model. In almost all systems, the Gamma[\mathcal{U}'_x]×Gamma[\mathcal{U}'] model, eq 35, is really necessary to describe very accurately at all isochores, from ideal gas to dense liquid, the system's thermal behavior over an extended and very large temperature range (up to $\sim 15T_c$). Only the hard core Yukawa fluid and water can be very well described by a single Gamma model over a considerable temperature range. This suggests some kind of inverse relation between the complexity of the molecular Hamiltonian and the complexity of the macroscopic energy distribution of the system.

The previously derived "perturbed Gamma state" model as used for the LJ fluid, is in fact just a good approximation to the more physical Gamma[\mathcal{U}'_x]×Gamma[\mathcal{U}'] model. In general, fluids are well described by a continuous mixture of (Gamma) distributions. However, in the case of systems involving large flexible molecules, e.g., proteins, the discrete (negative binomial) mixture of Gamma states (eq 44), might be used.^{16,52}

Molecular properties are (indirectly) reflected in the shape of the potential energy distribution, e.g., the skewness Δ_0 (eq 32): attractive van der Waals forces result in a left-skewed distribution; (continuous) repulsive forces superimpose a (strongly) right-skewed contribution that dominates at high density, and the presence of long-range electrostatic interactions reduces the asymmetry again at higher densities, resulting in a simpler, more Gaussian-like thermodynamics.

The Gamma[\mathcal{U}'_x]×Gamma[\mathcal{U}'] model, especially, may well serve as the basis of a complete theoretical density–temperature EOS, or be used to smooth and correlate raw experimental data, instead of via polynomial-like terms.

The Gamma distributions of the mixture are typically rather right-skewed, with the skewness parameter δ_0 close to unity (the harmonic limit). This suggests an interesting relation between the Gamma[\mathcal{U}'_x]×Gamma[\mathcal{U}'] QGE model and the (Gaussian) energy landscape picture of (supercooled) liquids and glasses, as well as macromolecules in solution. Work into this direction is in progress.

Finally, the multistate QGE models as presented here are also directly applicable to (chemical) mixtures, e.g., mixtures of LJ fluids or argon with methane. The QGE models can provide

the overall free energy and related thermodynamic functions, including, as shown very recently (ref 53), the partial molar properties.

Acknowledgment. This research was supported by the Training and Mobility of Researchers (TMR) Program of the EU, and by the Dutch Technology Foundation (STW). M.E.F.A. thanks Prof. Debenedetti for some reprints and stimulating discussions. We also thank Prof. Di Nola for useful discussions.

References and Notes

- (1) Sengers, J. V.; Kayser, R. F.; Peters, C. J.; White, H. J., Jr., Eds. *Equations of state for fluids and fluid mixtures*; Elsevier: Amsterdam, 2000.
- (2) Chapman, W. G.; Gubbins, K. E.; Jackson, G.; Radosz, M. *Fluid Phase Equilib.* **1989**, *52*, 31–38.
- (3) Chapman, W. G.; Gubbins, K. E.; Jackson, G.; Radosz, M. *Ind. Eng. Chem. Res.* **1990**, *29*, 1709–1721.
- (4) Setzmann, U.; Wagner, W. *Int. J. Thermophys.* **1989**, *10*, 1103.
- (5) Tegeler, C.; Span, R.; Wagner, W. *J. Phys. Chem. Ref. Data* **1999**, *28*, 779–849.
- (6) Setzmann, U.; Wagner, W. *J. Phys. Chem. Ref. Data* **1991**, *20*, 1061–1151.
- (7) Span, R.; Wagner, W. *J. Phys. Chem. Ref. Data* **1996**, *25*, 1509–1596.
- (8) Saul, A.; Wagner, W. *J. Phys. Chem. Ref. Data* **1989**, *18*, 1537–1564.
- (9) Amadei, A.; Apol, M. E. F.; Berendsen, H. J. C. *J. Chem. Phys.* **1997**, *106*, 1893–1912.
- (10) Amadei, A.; Apol, M. E. F.; Berendsen, H. J. C. *J. Chem. Phys.* **1998**, *109*, 3004–3016.
- (11) Apol, M. E. F. The Quasi-Gaussian Entropy Theory. Temperature dependence of thermodynamic properties using distribution functions. Ph.D. Thesis, Rijksuniversiteit Groningen, The Netherlands, 1997. Also available from: <http://docserver.ub.rug.nl/eldoc/dis/science/m.e.f.apol/>.
- (12) Apol, M. E. F.; Amadei, A.; Di Nola, A. *J. Chem. Phys.* **2002**, *116*, 4426–4436.
- (13) Amadei, A.; Apol, M. E. F.; Di Nola, A.; Berendsen, H. J. C. *J. Chem. Phys.* **1996**, *104*, 1560–1574.
- (14) Apol, M. E. F.; Amadei, A.; Berendsen, H. J. C. *J. Chem. Phys.* **1996**, *104*, 6665–6678.
- (15) Amadei, A.; Apol, M. E. F.; Chillemi, G.; Berendsen, H. J. C.; Di Nola, A. *Mol. Phys.* **1999**, *96*, 1469–1490.
- (16) Amadei, A.; Iacono, B.; Grego, S.; Chillemi, G.; Apol, M. E. F.; Paci, E.; Delfini, M.; Di Nola, A. *J. Phys. Chem. B* **2001**, *105*, 1834–1844.
- (17) Johnson, N. I.; Kotz, S.; Kemp, A. W. *Univariate discrete distributions*, 2nd ed; J. Wiley: New York, 1992.
- (18) Amadei, A. Theoretical Model for Fluid Thermodynamics based on the quasi-Gaussian Entropy Theory. Ph.D. Thesis, Rijksuniversiteit Groningen, The Netherlands, 1998. Also available from: <http://docserver.ub.rug.nl/eldoc/dis/science/a.amadei/>.
- (19) Roccatano, D.; Amadei, A.; Apol, M. E. F.; Di Nola, A.; Berendsen, H. J. C. *J. Chem. Phys.* **1998**, *109*, 6358–6363.
- (20) Patel, J. K.; Kapadia, C. H.; Owen, D. B. *Handbook of statistical distributions*; Marcel Dekker: New York, 1976.
- (21) Hummer, G.; Pratt, L. R.; García, A. E. *J. Am. Chem. Soc.* **1997**, *119*, 8523–8527.
- (22) Apol, M. E. F.; Amadei, A.; Berendsen, H. J. C.; Di Nola, A. *J. Chem. Phys.* **1999**, *111*, 4431–4441.
- (23) Johnson, N. I.; Kotz, S.; Balakrishnan, N. *Continuous univariate distributions*, 2nd ed; J. Wiley: New York, 1994; Vol. 1.
- (24) Duh, D.-M.; Mier-y-Terán, L. *Mol. Phys.* **1997**, *90*, 373–379.
- (25) Henderson, D.; Blum, L.; Nowoyta, J. P. *J. Chem. Phys.* **1995**, *102*, 4973–4975.
- (26) Henderson, D.; Waisman, E.; Lebowitz, J. L.; Blum, L. *Mol. Phys.* **1978**, *35*, 241–255.
- (27) Levelt Sengers, J. M. H. *Fluid Phase Equilib.* **1999**, *158–160*, 3–17.
- (28) Wyczalkowska, A. K.; Anisimov, M. A.; Sengers, J. V. *Fluid Phase Equilib.* **1999**, *158–160*, 523–535.
- (29) Kiselev, S. B.; Ely, J. F.; Adidharma, H.; Radosz, M. *Fluid Phase Equilib.* **2001**, *183–184*, 53–64.
- (30) Lemmon, E. W.; McLinden, M. O.; Friend, D. G. Thermophysical Properties of Fluid Systems. *NIST Chemistry Webbook*; National Institute of Standards and Technology: Gaithersburg MD, 2001; chapter X.
- (31) Tillner-Roth, R.; Harms-Watzenberg, F.; Baehr, H. D. *DKV-Tagungsbericht* **1993**, *20*, 167–181.
- (32) Berendsen, H. J. C.; Grigera, J. R.; Straatsma, T. P. *J. Phys. Chem.* **1987**, *91*, 6269–6271.
- (33) Jedlovsky, P.; Richards, J. J. *J. Chem. Phys.* **1999**, *110*, 8019–8031.

- (34) van der Spoel, D.; van Maaren, P. J.; Berendsen, H. J. C. *J. Chem. Phys.* **1998**, *108*, 10220–10230.
- (35) Zhu, S.-B.; Sing, S.; Robinson, G. W. *Adv. Chem. Phys.* **1994**, *85*, 627–732.
- (36) Berendsen, H. J. C.; van der Spoel, D.; van Drunen, R. *Comput. Phys. Comm.* **1995**, *91*, 43–56.
- (37) Lindahl, E.; Hess, B.; van der Spoel, D. *J. Mol. Model.* **2001**, *7*, 306–317.
- (38) van der Spoel, D.; van Buuren, A. R.; Apol, E.; Meulenhoff, P. J.; Tieleman, D. P.; Sijbers, A. L. T. M.; Hess, B.; Feenstra, K. A.; Lindahl, E.; van Drunen, R.; Berendsen, H. J. C. *Gromacs User Manual version 3.0*; Nijenborgh 4, 9747 AG Groningen, The Netherlands, 2001.
- (39) Darden, T.; York, D.; Pedersen, L. *J. Chem. Phys.* **1993**, *98*, 10089–10092.
- (40) Essmann, U.; Perera, L.; Berkowitz, M. L.; Darden, T.; Lee, H.; Pedersen, L. G. *J. Chem. Phys.* **1995**, *103*, 8577–8592.
- (41) Berendsen, H. J. C.; Postma, J. P. M.; van Gunsteren, W. F.; Di Nola, A.; Haak, J. R. *J. Chem. Phys.* **1984**, *81*, 3684–3690.
- (42) Evans, D. J.; Morris, G. P. *Comput. Phys. Rep.* **1984**, *1*, 297.
- (43) Morishita, T. *J. Chem. Phys.* **2000**, *113*, 2976–2982.
- (44) Miyamoto, S.; Kollman, P. A. *J. Comput. Chem.* **1992**, *13*, 952–962.
- (45) Allen, M. P.; Tildesley, D. J. *Computer simulation of liquids*; Oxford University Press: Oxford, U.K., 1989.
- (46) Straatsma, T. P.; Berendsen, H. J. C.; Stam, A. J. *Mol. Phys.* **1986**, *57*, 89.
- (47) Bishop, M.; Frinks, S. J. *J. Chem. Phys.* **1987**, *87*, 3675.
- (48) Stillinger, F. H. *Science* **1995**, *267*, 1935–1939.
- (49) Debenedetti, P. G.; Stillinger, F. H.; Truskett, T. M.; Roberts, C. *J. J. Phys. Chem. B* **1999**, *103*, 7390–7397.
- (50) Debenedetti, P. G.; Truskett, T. M.; Lewis, C. P.; Stillinger, F. H. *Adv. Chem. Eng.* **2001**, *28*, 21–79.
- (51) Amadei, A.; de Groot, B. L.; Ceruso, M. A.; Paci, M.; Di Nola, A.; Berendsen, H. *Proteins: Struct., Funct. Genet.* **1999**, *35*, 283–292.
- (52) Roccatano, D.; Di Nola, A.; Apol, M. E. F.; Amadei, A. Manuscript in preparation.
- (53) D'Alessandro, M.; D'Abramo, M.; Brancato, G.; Di Nola, A.; Amadei, A. *J. Phys. Chem. B* **2002**, *106*, 11843–11848.